Effect of Tacticity on Coil Dimensions and Thermodynamic Properties of Polypropylene

Todd D. Jones, Kimberly A. Chaffin,† and Frank S. Bates*

Department of Chemical Engineering and Materials Science, University of Minnesota, Minneapolis, Minnesota 55455

B. K. Annis, E. W. Hagaman, Man-Ho Kim, and George D. Wignall

Oak Ridge National Laboratory, Oak Ridge, Tennessee 37831-6393

W. Fan and R. Waymouth

Department of Chemistry, Stanford University, Stanford, California 94305-5080

Received August 29, 2001

ABSTRACT: Small-angle neutron scattering (SANS) has been used to measure the chain dimensions of syndiotactic polypropylene (*s*-PP) in the melt, using mixtures of ^{1}H- and ^{2}D-labeled molecules. This leads to a segment length 7.6 Å normalized to a four-carbon repeat unit, which is in excellent agreement with a prediction based on a correlation of chain conformation and the plateau modulus obtained from rheology. The *s*-PP segment length is substantially higher than the values of 6.2 Å previously obtained for isotactic polypropylene (*i*-PP) in the melt and 5.6 Å in a low-molecular-weight "polymeric solvent". We have also studied its effect on the thermodynamics of polyolefin blends by investigating the miscibility of *s*-PP with a range of atactic poly(ethylene/ethylethyelene) (PEE*x*) random copolymers, with *x*% ethylethylene, and comparing this with *i*-PP. The miscibility "window" of *i*-PP with PEE*x* ranges from $x = 63-96$% ethylethylene, while that of *s*-PP is shifted to $x = 53-73$%, in qualitative agreement with the concept that conformational symmetry matching favors miscibility. We have also performed a complementary measurement of the melt coil dimensions of *s*-PP, using a low-molecular-weight PEE*x* "polymeric solvent" similar to that previously employed for *i*-PP. A fit of the *s*-PP/PEE71 blend scattering yielded a segment length of 8.1 Å, supporting the previous finding that the coil dimensions of *s*-PP are substantially higher than *i*-PP. These results emphasize the important influence of tacticity on the chain dimensions and thermodynamic properties in polyolefin systems.

Introduction

Polypropylene serves a wide variety of commercial uses, being one of the four major commodity polymers.[1] However, the limitations on its synthesis mean that making molecules of well-controlled architecture, such as monodisperse materials or block copolymers, is difficult. Atactic polyolefins, including polypropylene, can be synthesized indirectly through anionic polymerization of a variety of diene monomers, followed by saturation of the residual double bonds. However, tactic PP cannot be synthesized by this method, being restricted to Ziegler−Natta or metallocene catalysis. Given the chemical similarity of the various polyolefins, one might expect them to form one-phase mixtures. In fact, relatively small differences give large changes in blend thermodynamics. For example, polyethylene and polypropylene are immiscible at essentially all conditions, as are many other polyolefins.

Polyolefins have been extensively studied as models for understanding phase behavior in polymer blends. Because of the absence of more complex functional groups, the thermodynamics of polyolefin blends are governed only by dispersive interactions between the components. Despite the comparative simplicity of these interactions, a number of complex behaviors have been reported in amorphous blends of hydrocarbon polymers, including "deuterium swap" effects and "irregular mixing".[2−9] These results suggest that factors in addition to simple dispersive interactions are required to completely describe polymer phase behavior, even for these simple polymers. Initial research by other groups has focused primarily on amorphous hydrocarbon polymers prepared from dienes. Amorphous materials can be studied over a wide range of temperatures, from the glass transition temperature until they decompose. In addition, these materials can be easily deuterated during synthesis, providing contrast for neutron scattering to determine the chain configuration and the Flory−Huggins interaction parameter, χ.

While amorphous hydrocarbon polymers are interesting model materials, crystalline polyolefins are more important from a commercial viewpoint due to their mechanical properties. The complexity of phase behavior previously reported in amorphous hydrocarbon polymers suggests that small changes in structure could have a large effect on phase behavior of crystalline systems. On this basis, tacticity can play an important role in governing polyolefin blend behavior. These effects have not previously been examined using small-angle neutron scattering. Polyethylene does not have inherent tacticity, but isotactic (*i*-PP) and syndiotactic (*s*-PP) polypropylene are now commercially available. While *i*-PP has been examined by a variety of authors, and its molecular properties are now well-known,[10−12] only recently has the advent of metallocene catalysis allowed preparation of large quantities of *s*-PP. *s*-PP has a significantly lower

† Current address: Medtronic, Inc., Materials and Biosciences Center, Brookyln Center, MN 55430.
* Corresponding author.

10.1021/ma011547g CCC: $22.00
Published on Web 05/15/2002

Table 1. Characteristics of Samples

polymer name	M_w (g/mol)	M_w/M_n	supplier	% [rrrr]
s-PP	180 000	2.2	Fina	86.3
s-PPh	179 000	2.2	Stanford	90
s-PPd	353 000	2.0	Stanford	89.7
i-PP1	70 000	2.4	Exxon	
i-PP2	120 000	2.4	Exxon	
i-PP3	91 000	2.0	Exxon	

melting point than *i*-PP (~135 and 175 °C, respectively) as well as a different crystal structure,[13,14] while its mechanical properties are also altered, having a tensile strength comparable to *i*-PP but a lower modulus.[15] However, these observations are less surprising than the different melt properties of *s*-PP, including a higher viscosity for a given molecular weight and a much higher plateau modulus.[16]

These differences in properties of polymers with nearly identical chemical structures emphasize the importance of understanding structural effects in polyolefin blends. We have studied the effect of tacticity on both chain conformation and melt miscibility by using $^1H/^2D$-substituted melts for *s*PP and a series of blends of isotactic or sydiotactic PP with poly(ethylene-*co*-butene) model polyolefins in order to provide insight into the role these factors play in blend thermodynamics.

Experimental Section

Materials. A series of isotactic polypropylenes were provided by Exxon Chemical, and hydrogenous syndiotactic polypropylene was supplied by Fina Chemical. These polymers were used as received, and their properties as reported by the manufacturer are summarized in Table 1. Molecular weight and polydispersity were confirmed within 10% by high-temperature GPC measurements in trichlorobenzene. The synthesis of a series of polybutadienes with amounts of 1,2 addition ranging from 41% to 96% has been previously described,[12] along with their characterization by ^1H NMR and density gradient methods. Molecular weights and polydispersities were obtained by combined GPC light scattering using a DAWN LALLS detector and a Wyatt differential refractometer, with the exception of PBD53, for which universal calibration from polystyrene standards was used. Values of d*n*/d*c* were measured with a differential refractometer using a series of 10 solutions in tetrahydrofuran ranging in concentration from 0.2 to 2 mg/mL. Low-molecular-weight mostly deuterated polybutadienes were also prepared as described in the literature. Polybutadienes were catalytically hydrogenated or deuterated under standard conditions to form the corresponding ethylene/ethylethylene copolymer. The properties of these polymers are summarized in Table 2.

The protiated (*s*-PPh) and deuterated (*s*-PPd) *s*-PP were prepared by metallocene polymerization. All manipulations with organometallic compounds were conducted using standard Schlenk and drybox techniques. The metallocene $Me_2C(Cp)(Flu)ZrMe_2$ was synthesized according to literature procedures.[17] Toluene was passed through two purification columns packed with activated alumina and supported copper catalysts. Methylaluminoxane (MAO), type 3A, purchased from Akzo, was dried in vacuo prior to use. Polymer grade propene gas was purchased from Matheson and purified by passage through two columns packed with activated alumina and supported copper catalyst. Propene-d_6 (98% purity) was purchased from Cambridge Isotope Lab and purified over methylaluminoxane for 2 days.

The polymerization of propene used the MAO-activated metallocene catalyst, $Me_2C(Cp)(Flu)ZrCl_2$. A 300 mL stainless steel reactor equipped with a mechanical stirrer was evacuated, purged three times with Ar and propene gas by pressurizing and venting, and charged with 80 mL of toluene solution containing 290 mg of MAO. The reactor was connected to the propene gas tank with 35 psig propene pressure and was kept constant at 20 °C throughout the polymerization.

Table 2. Properties of Hydrogenated Model Polyolefins

polymer	$\rho_h{}^a$ (g/cm^3, 25 °C)	$\rho_d{}^a$ (g/cm^3, 25 °C)	$n_D{}^a$	$N_w{}^a$	b^a (Å, 180 °C)
PEE41	0.8569	0.9077	3.19	972	6.8
PEE46	0.8570	0.8935	2.32	1053	6.9
PEE53	0.8588	0.9115	3.45	724	7.2
PEE58	0.8597	0.9116	3.23	1686	6.1
PEE63	0.8607	0.9057	3.01	1294	6.0
PEE66	0.8614	0.9102	3.10	1286	6.0
PEE73	0.8650	0.8979	2.07	1133	5.4
PEE83	0.8688	0.9105	2.62	1434	5.3
PEE90	0.8688	0.9068	2.38	905	5.2
PEE96	0.8688	0.9105	2.68	878	5.1
PEE90-d_6		0.9570	6.3	171	5.2[b]
PEE73-d_6		0.9643	6.5	124	5.7[b]
PEE71-d_6		0.9569	6.1	350	5.6[b]

[a] ρ_h and ρ_d are densities of hydrogenated and deuterated polymers, respectively. n_D is number of deuterium atoms per repeat unit. N_w is weight-average degree of polymerization. *b* is statistical segment length. [b] Values taken as equal to higher molecular weight samples.

After 30 min equilibration, an injection tube containing 20 mL of toluene solution of metallocene (2×10^{-6} mol) was taken out of the drybox and injected to the reactor. The polymerization was run for 30 min and stopped by injection of 5 mL of methanol solution. The polymer was stirred in 300 mL of methanol containing 5% concentrated hydrochloric acid, rinsed with methanol, and dried at 40 °C in vacuo overnight. Yield: 2.24 g (white powder). Productivity: 2240 kg/(mol h mol Zr). Values of $M_w = 179\,000$ kg/mol and $M_w/M_n = 2.2$ were obtained by high-temperature GPC and were measured by BP Amoco.

The polymerization of propene-d_6 was identical to that of propene, with the exception that the pressure/temperature were 18 psig/20 °C, the yield/productivity were 0.758/758 kg/(mol h mol Zr), and M_w and M_w/M_n were 353 000 and 2.0. The molecular weight of polypropylene-d_6 is higher than that of polypropylene (see Table 1). Carbon 13 NMR measurements (see below) on the protiated sample established a racemic pentad content of 90%.

NMR Spectroscopy. The ^{13}C NMR spectra were recorded on a Bruker Avance NMR spectrometer operating at 9.4 T. Carbon spectra of the polymers were acquired using conventional $\{^nH\}^{13}C$ single-pulse excitation experiments ($n = 1, 2$) with a 4.0 μs 90° pulse and 5 s recycle decay. Carbon spectra were acquired at 100.613 MHz. Free induction decays, collected in 64K points, gave frequency domain spectra with 0.315 Hz/point digital resolution. The FID was apodized with a decaying exponential function, which broadened the lines 1 Hz. The broad-band decoupling irradiation frequency was 400.132 007 and 61.422 910 6 MHz for ^1H and ^2H, respectively, with a power of 7−8 W. Spectra were acquired at 405 ± 5 K in an unlocked mode on samples dissolved in *o*-dichlorobenzene (ODCB): ^1H PP, 26.2 mg in 0.55 mL of ODCB; ^2H PP, 38.1 mg in 0.80 mL of ODCB. Chemical shifts are expressed on the TMS scale ($\delta = 0$ ppm) using the C(4) resonance of ODCB as a secondary reference ($\delta = 127.9$ ppm). ^{13}C NMR on the Fina s-PP sample indicated a racemic pentad content of 86.3%, substantially lower than the value of 93% provided by the manufacturer. However, the two values are felt to be within the uncertainty of the experiment. Using group additivity to predict chemical shifts, as described by Tulloch and Mazurek,[18] the peaks for the deuterated s-PP sample were predicted. In addition, the spectrum contains several closely spaced resonances near 19.2 ppm, partially overlapping the rrrm pentad sequence resonance that likely reflect heptad configurational sequences, as has been noted in the rr dyad sequence region of the methyl resonance of PP.[19] On the basis of these assignments, a racemic pentad content of 89.7% was measured for the deuterated s-PP.

Neutron Scattering. Crystalline−amorphous blends of polypropylene with deuterium-labeled PEE*x* were prepared by dissolving the polymers in decahydronaphthalene (10% w/v), followed by precipitation into dry ice/methanol. The resulting blends were vacuum-dried, pressed at 200 °C under vacuum,

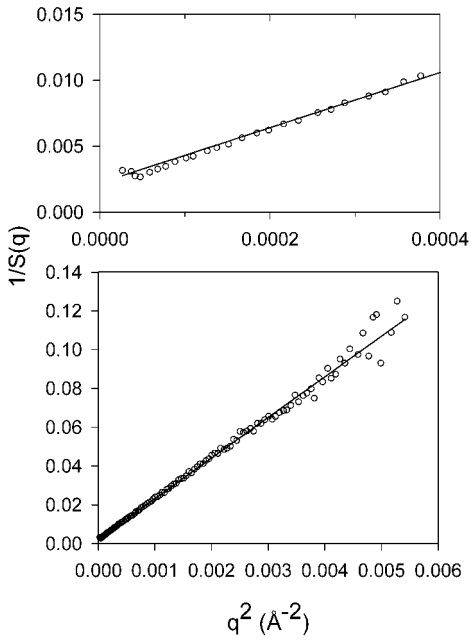

Figure 1. 50H/50D sPP melt (○). Solid line is a least-squares fit to eq 2. Upper plot is an expansion of the lower left corner of the lower plot.

and sealed into quartz cells. Crystalline−amorphous blends of polypropylene with low-molecular-weight PEE90-d_6 or PEE73-d_6 were prepared by loading the sample into a quartz necked cell containing a small steel stirbar and less than 1% of di-*tert*-butylhydroxytoluene (BHT) as a thermal stabilizer. The cell was subsequently sealed with a Teflon plug and stirred for 48 h at 200 °C in order to homogenize the mixture.

Most of the neutron scattering measurements involving the random copolymers were undertaken on the NIST/Exxon/University of Minnesota 30 m SANS instrument at NIST in Gaithersburg, MD, while experiments on s-PP homopolymer melts were performed on the W. C. Koehler SANS facility[20] at Oak Ridge National Laboratory (ORNL). In addition, samples of *s*-PP dissolved in low-molecular-weight "polymeric solvents" were run at both ORNL and NIST in order to determine the consistency of our measurements.

The ORNL SANS facility has a 64 × 64 cm^2 area detector with element size ∼1 cm^2 and a wavelength $\lambda = 4.75$ Å; $\Delta\lambda/\lambda \sim 5\%$. Sample-to-detector distances of 7.9 and 3.3 m were used for the small- and intermediate-angle measurements to give q ranges of $0.008 < q = 4\pi\lambda^{-1}\sin(\theta/2) < 0.08$ Å^{-1} and $0.02 < q < 0.20$ Å^{-1}, respectively, where θ is the scattering angle. The data were corrected for detector efficiency and instrumental backgrounds (including the "beam-blocked" background and the "empty cell" signal) and detector efficiency on a cell-by-cell basis, prior to radial averaging. The net intensities were converted to an absolute (±4%) differential cross section per unit sample volume [in units of cm^{-1}] by comparison with precalibrated secondary standards.[21] Details of transmission measurements and correction procedures for instrumental and incoherent backgrounds (∼1 cm^{-1}) have been given previously.[22] The samples were maintained at 180 °C.

At NIST, a wavelength of 7 Å was used with 9% wavelength spread, with sample-to-detector distances of 6, 10, or 15 m and a typical sample temperature of 185 °C. Sample transmissions were measured before each scattering experiment. In addition to sample transmission, data were corrected for background radiation, sample thickness, and detector sensitivity. As at ORNL, the data were azimuthally averaged as a function of the scattering vector q and converted to an absolute scale via a precalibrated irradiated Al-7 sample.[21]

Rheology. Rheology measurements were carried out on *i*-PP and *s*-PP using a Rheometrics DSR stress rheometer with a 25 mm parallel plate fixture at temperatures ranging from 170 to 210 °C. The values of G' and G'' were measured as a function of frequency. The data for *i*-PP and *s*-PP were then directly compared under similar conditions.

Results and Analysis

Isotopic Blends of Syndiotactic Polypropylene. To investigate the effect of tacticity on polyolefin miscibility, it was first necessary to measure the segment length, and the most direct way to do this was via blends of ^{1}H- and ^{2}D-labeled *s*-PP. In addition, we have performed complementary measurements using a low-molecular-weight "polymeric solvent" as in previous measurements on *i*-PP[12] (see below). Standard and perdeuterated *s*-PP were prepared and blended as described above, and the SANS data (obtained at ORNL) on *s*-PP h/d melts were analyzed in several different ways, all of which gave good agreement. The 50/50 h/d sample was measured with a 7.9 m sample-to-detector distance, giving a q range of $0.008 < q < 0.08$ Å^{-1}. The data were corrected for incoherent background scattering prior to analysis. The coherent small-angle scattering from an amorphous single-phase blend can be fit using de Gennes' random phase approximation[23] for polydisperse components using the following equations:[12,24]

$$I_{\mathrm{coh}}(q) = \left(\frac{\sum_i b}{v_i} - \frac{\sum_j b}{v_j}\right)^2 S(q)$$

$$\frac{1}{S(q)} = \frac{1}{N_i\phi_i g_{Pi}(x_{ni})} + \frac{1}{N_j\phi_j g_{Pj}(x_{nj})} - 2\chi_{ij}$$

$$g_{Pi}(x_{ni}) = (2/x_{ni}^2)\left[x_{ni} - 1 + \left(1 + \frac{x_{ni}}{k_i}\right)^{-k_i}\right] \qquad (1)$$

$$x_{ni} = q^2 R_{\mathrm{g},ni}^2$$

where $\sum_i b$ is the sum of the coherent scattering lengths of a segment of component i, v_i is its volume, g_{Pi} is the polydisperse Debye function, $R_{\mathrm{g},ni}$ is the number-average radius of gyration, and $k_i = (N_{\mathrm{w}i}/N_{\mathrm{n}i} - 1)^{-1}$ describes the polydispersity, based on a Schultz−Zimm distribution function for the ith component. In the case of a narrow polydispersity component, such as a model polyolefin, g_{Pi} is replaced by the Debye coil function for a monodisperse polymer.

In the limit of low q, Boué et al.[25] approximated eq 1 for two polydisperse components as

$$S(q)^{-1} = \frac{1}{N_{\mathrm{w}D}\phi_{\mathrm{D}}} + \frac{1}{N_{\mathrm{w}H}\phi_{\mathrm{H}}} - 2\chi_{\mathrm{hd}} + \frac{q^2b^2}{18}\left[\frac{N_{\mathrm{z}D}}{N_{\mathrm{w}D}\phi_{\mathrm{D}}} + \frac{N_{\mathrm{z}H}}{N_{\mathrm{w}H}\phi_{\mathrm{H}}}\right] \qquad (2)$$

where $N_{\mathrm{w}i}$ and N_{zi} are the weight- and z-average degrees of polymerization, respectively, and b is the segment length. From the Schultz−Zimm distribution, $N_z = 2N_{\mathrm{w}} - N_{\mathrm{n}}$, where N_{n} is the number-average, eq 2 may be written

$$S(q)^{-1} = \frac{1}{N_{\mathrm{w}D}\phi_{\mathrm{D}}} + \frac{1}{N_{\mathrm{w}H}\phi_{\mathrm{H}}} - 2\chi_{\mathrm{hd}} + \frac{q^2b^2}{18}\left[\frac{2y_{\mathrm{D}} - 1}{y_{\mathrm{D}}\phi_{\mathrm{D}}} + \frac{2y_{\mathrm{H}} - 1}{y_{\mathrm{H}}\phi_{\mathrm{H}}}\right] \qquad (3)$$

where $y_i = N_{\mathrm{w}i}/N_{\mathrm{n}i}$. The segment length is then obtained from the slope of a $S(q)^{-1}$ vs q^2 plot. Figure 1 shows a

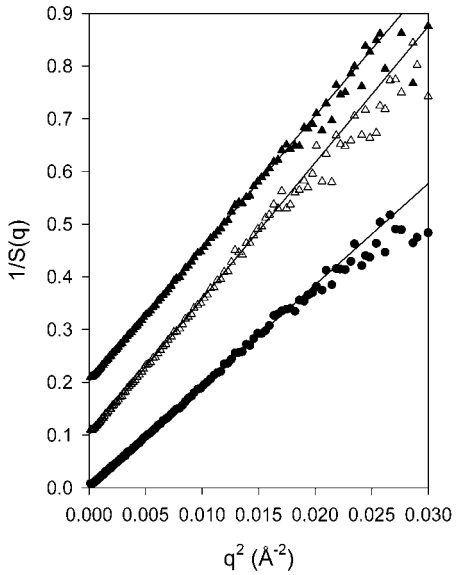

Figure 2. Comparison of intermediate q range approximation for *s*-PPh/*s*-PPd melts: 50H/50D (●); 75H/25D (△); 25H/75D (▲).

plot of the data and the fit to the data in this form. The resulting value for a four carbon segment length is 7.6 ± 0.3 Å.

The melt data for the three compositions taken with a 3.3 m sample-to-detector distance [$0.02 < q < 0.20$ Å^{-1}] were analyzed in two ways. The first made use of the approximation to eq 1 in the intermediate q range,[25]

$$S(q)^{-1} = \frac{1}{N_{nD}\phi_D} + \frac{1}{N_{nH}\phi_H} - 2\chi_{hd} + \frac{q^2b^2}{12}\frac{1}{\phi_D\phi_H} \quad (4)$$

In this case the slope of the $S(q)^{-1}$ vs q^2 plot is independent of the polydispersity. The results for the three compositions are shown in Figure 2. The average of the segment lengths was 7.6 ± 0.3 Å, in excellent agreement with the low-q result for the 50/50 h/d sample.

In the limit that the q^2 dominates, a plot of $q^2I(q)$ vs q should come to a constant value referred to as the Kratky plateau. The segment length is then obtained from

$$b^2 = \left(\frac{{b_1}^2}{v_1\phi_1} + \frac{{b_2}^2}{v_2\phi_2}\right) = \frac{12\phi_1\phi_2\left(\frac{\sum_i b}{v_i} - \frac{\sum_j b}{v_j}\right)^2}{(q^2I(q))_{plateau}} \quad (5)$$

For the *s*-PP h/d blends isotopic changes in the segment volumes and lengths are considered to be negligible, and the results for the three melts are shown in Figure 3. From the Kratky plateaus an average of 7.6 ± 0.3 Å is once again found for a four-carbon segment length.

The statistical segment length of s-PP also may be determined from measurements in low-molecular-weight deuterated "polymeric solvents", as described in our previous paper.[12] However, initial attempts to use the PEE90d6 material described in that publication were unsuccessful, as *s*-PP was immiscible at accessible temperatures with that material. We were able to disperse *s*-PP in low molecular weight deuterated PEE73-d_6, which was synthesized and characterized as described previously.[12] Results for a sample composed of FINA *s*-PP ($\phi = 0.131$) in PEE73-d_6 and a sample of

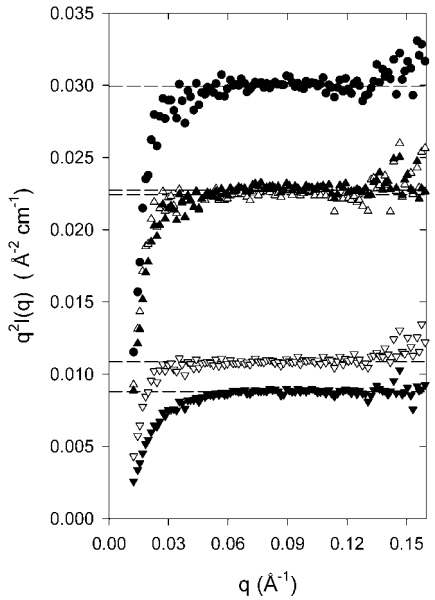

Figure 3. Comparison of Kratky plots: 50H/50D sPP melt (●); 75H/25D sPP melt (△); 25H/75D sPP melt (▲); FINA sPP/PEE73-d_6−7.5, $\phi = 0.131$ (▼); HsPP/PEE73-d_6−20, $\phi = 0.145$ (▽).

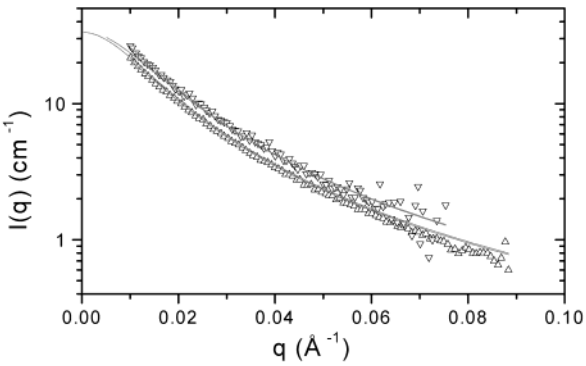

Figure 4. Simultaneous fit of scattering patterns from blends of s-PP and PEE73-d_6 with a PP volume fraction of (△) 0.108 and (▽) 0.131. The lines through the data represent a simultaneous nonlinear least-squares best fit, giving a statistical segment length of 8.1 Å at 185 °C.

s-PPh ($\phi = 0.145$) in PEE71-d_6 measured at the ORNL facilities are also shown in Figure 3. Taking $v_1 = v_2 = 120$ Å^3 for a four-carbon segment and b for PEE 71 and PEE73 equal to 5.4 Å from Table 2, the resulting segment lengths for *s*-PP are then 8.0 ±0.3 and 6.9 ± 0.3 Å, respectively. Averaging these two determinations gives a value of 7.45 Å, which is within the error limits (7.6 ± 0.3 Å) of the homopolymer melt determinations, both in the low- and intermediate-q ranges. An independent measurement using two samples of FINA s-PP in PEE73-d_6 ($\phi = 0.131$, 0.108) yielded similar results, as shown in Figure 4. In this case, the $\phi = 0.131$ sample was run at the ORNL facilities, while the $\phi = 0.108$ sample was run at the NIST facilities. Simultaneous fitting of the scattering data using the structure factor described in eq 1 yielded a statistical segment length for s-PP of 8.1 ± 0.3 Å, which agrees within error with the value of 7.6 ± 0.3 Å from homopolymer melt determinations

Blends of Syndiotactic Polypropylene with Model Polyolefins. Our initial attempts to disperse *s*-PP in low-molecular-weight PEE90 indicated that its miscibility characteristics were significantly different

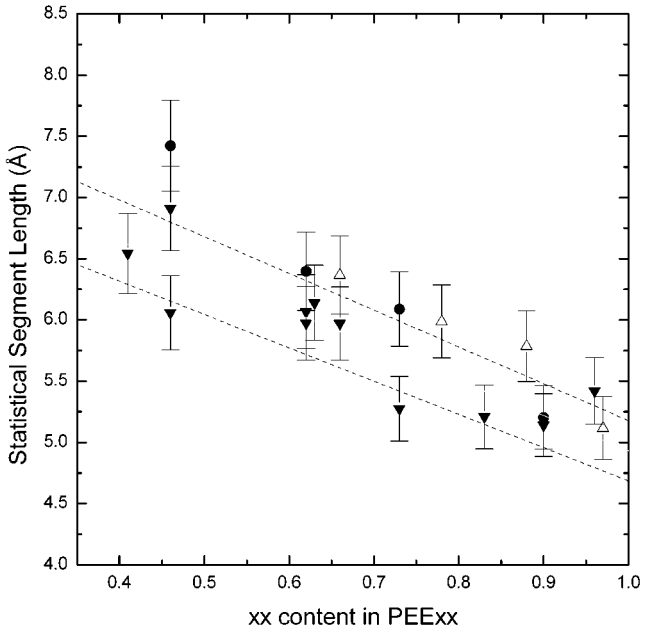

Figure 5. Comparison of statistical segment lengths from various experimental methods. Open symbols represent extrapolations in temperature from the work of Graessley et al.[27] Solid symbols (●, ▼) represent our original results[10] and more recent data, respectively. The solid line represents a linear least-squares fit to all of the data.

Table 3. Measured Values of χ at 185 °C for Polypropylene Blended with PEE*x*-*d*

PEE*x* microstructure	χ, s-PP ($\times 10^4$)	PEE*x* microstructure	χ, s-PP ($\times 10^4$)
41	−	66	8.3 ± 1.6
46	imm	73	6.7 ± 1.7
53	14.6 ± 4.0	82	imm
58	5.2 ± 1.5	90	imm
63	7.3 ± 1.3	96	−

from *i*-PP. To determine which microstructures of PEE*x*, if any, were miscible with *s*-PP, we blended it with eight PEE*x*-*d* model polyolefins of copolymer composition varying from 46 to 90% ethylethylene (Table 3). This series included PEE63-*d*, a replacement for PEE62-*d* from our previous publication,[12] of which we had insufficient material. Volume fraction and contrast factors were calculated as described previously[12] based on the densities listed in Table 2. Statistical segment lengths of the model PEE*x*-*d* polyolefins were determined by matched-pair isotope-labeling experiments. These values were compared with both our previous results and the measurements of Graessley et al.[2−9] after correcting for temperature. As seen in Figure 5, a plot of statistical segment length vs EE content can be approximated by a straight line. Within the experimental limits of our technique and extrapolation of statistical segment lengths from different temperatures, our data and others agree reasonably well.

After fitting the data to a scattering function based on a monodisperse−polydisperse RPA structure factor (eq 1) by a nonlinear least-squares fitting method,[12] we found that *s*-PP of this molecular weight was miscible with PEE53-*d*, PEE58-*d*, PEE63-*d*, PEE66-*d*, and PEE73-*d* at 185 °C. These assignments were confirmed by visual observation of sample clarity in the melt. All other deuterium-labeled polyolefins in this study were immiscible, based on the measured scattering profiles, and are clearly outside the χ-window, as shown in Figure 6. Allowing both χ and the statistical segment length of *s*-PP to vary for the five miscible high-molecular-weight polyolefins (PEE53−73-*d*) gave values in the range 8.3−9.8 Å for b_{s-PP}, somewhat larger than the values measured in either the isotopic blends or the low-molecular-weight model polyolefin blends. Values of χ (Table 3) obtained from fits to the data with b_{s-PP} fixed at 7.6 Å show the expected behavior, with generally higher values observed near the edge of the miscibility window. These results confirm that the statistical segment length of *s*-PP is increased relative to *i*-PP. In addition, the window of miscibility in PEE*x* blends is shifted significantly from *i*-PP, which forms single-phase blends with PEE63 through PEE96 at similar temperatures.[12,26]

Discussion

The *s*-PP segment lengths measured in the melt and in a matrix of the PEE*x* copolymer are both significantly greater than that of either *i*-PP or *a*-PP.[11] The slightly higher value of *b* measured in melt blends with PEE*x*-*d* may reflect the fact that *s*-PP is immiscible with high-molecular-weight PEE over much of the composition range studied. Thus, these blends may be close to a phase boundary for the five samples that were judged to be miscible (PEE53-*d*−PEE73-*d*). In addition, the low-molecular-weight matrix (PEE71-d_6) may act as a good solvent and slightly swell the chain dimensions and hence give a segment length slightly greater (8.1 Å) than that measured in the melt (7.6 Å). However, both independent determinations confirm that the statistical segment of *s*-PP is significantly greater than that of either *i*-PP or *a*-PP.

While departures from the RPA fits are seen at the lowest q values in scattering involving the PEEx materials (Figure 6), the general form of the scattering is inconsistent with the onset of phase segregation. In the case of phase segregation, the scattering at higher q values would not fit within the χ window, as is seen in Figure 6a,g. Instead, we attribute this upturn to the presence catalyst residue in the PEEx materials. Since these are prepared by catalytic hydrogenation, followed by filtration through a 0.2 μm membrane, it is likely that particles smaller than 0.2 μm in diameter would not be removed. This type of scattering has been reported previously and attributed to this cause.[12,27]

An alternate way of summarizing the melt data is to convert the statistical segment length to the ratio of the rms radius of gyration and the molecular weight. A value of $\langle R_g^2\rangle/M = 0.172 \pm 0.013$ Å^2 mol g^{-1} results. For *i*-PP, Ballard et al.[10] obtained a value of $\langle R_g^2\rangle/M = 0.12$. The characteristic ratio, C_∞, can be expressed as $C_\infty = 6(\langle R_g^2\rangle/M)m_0 l_0^{-2}$, where m_0 is the average molecular weight of a backbone bond with length l_0. The ratio of C_∞ for *s*-PP to that for *i*-PP is then 1.4. This is in reasonable agreement with a value of 1.5 calculated by Pütz et al.[28] from PRISM theory for chains of 96 monomers. Molecular dynamics simulations also have predicted that *s*-PP will have a significantly extended chain conformation in the melt relative to *i*-PP.[29] In effect, the alternating position of the methyl groups leads to the trans configuration of the chain being more stable. As a result, the *s*-PP chain is stiffer, and the difference in statistical segment length and miscibility between *s*-PP and *i*-PP suggests that local chain packing and stereochemistry effects play a large role in determining polymer properties.

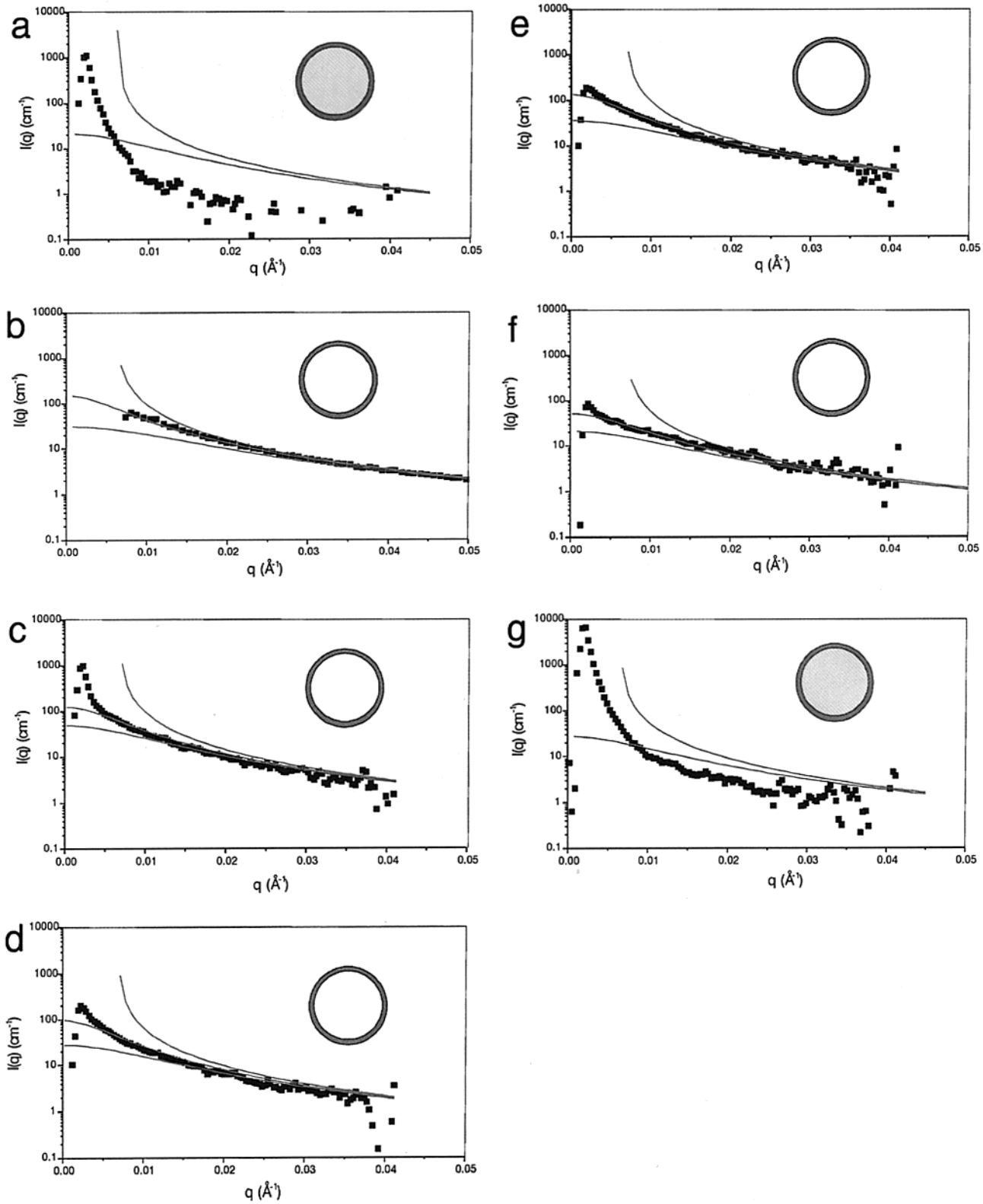

Figure 6. Miscibility of *s*-PP with PEE*x* of various microstructures. These PEE*x* materials are (a) PEE46-*d*, (b) PEE53-*d*, (c) PEE58-*d*, (d) PEE63-*d*, (e) PEE66-*d*, (f) PEE73-*d*, and (g) PEE83-*d*. As expected, *s*-PP forms a miscibility window with the PEE*x*. This window ranges from PEE58-*d* to PEE73-*d*, based on the scattering patterns. As before, the line through the data represents the best nonlinear least-squares fit where it is possible, while the upper and low bounds represent the limits imposed for $\chi = 0$ and $\chi = \chi_s$. Samples that were not transparent in the melt are shown with gray circles while transparent samples are shown as white.

On examining our blend results, we see that the miscibility window of *s*-PP with model polyolefins is significantly different from *i*-PP. Using a larger series of model polyolefins, we have first determined the miscibility window for *i*-PP more precisely than our previous report.[12] For PP3045, the miscibility window ranges from PEE63-*d* to PEE96-*d*. In agreement with the Bates and Fredrickson hypothesis[30] regarding additional entropic contributions from statistical segment length differences, the PEE*x* structures forming the

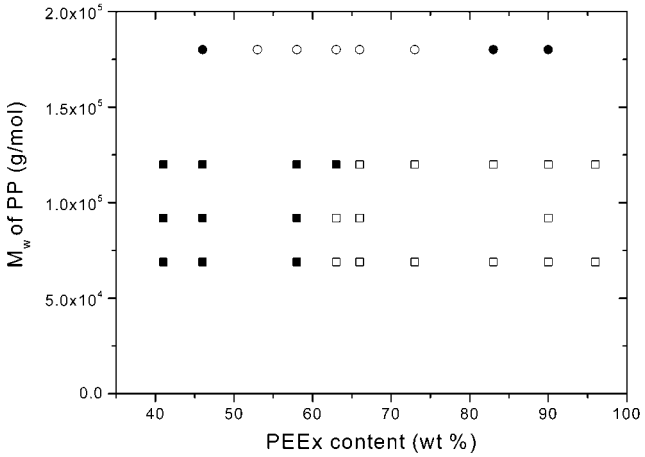

Figure 7. Miscibility window of *i*-PP (■, □)[26] and *s*-PP (●, ○) with PEE*x*, as determined from neutron scattering. Open symbols represent miscibility. As molecular weight is increased, the miscibility window narrows. As tacticity is changed from isotactic to syndiotactic, the miscibility window shifts from a center at PEE78 to a center at PEE65.

boundary of the miscibility window are nearly symmetric in statistical segment length around *i*-PP.

On switching from isotactic to syndiotactic polypropylene there is a significant change in mixing properties. Prior reports have indicated that *i*-PP and *s*-PP are immiscible in the melt and do not cocrystallize.[13] PVT measurements have also shown that *s*-PP and *i*-PP have different cohesive energy densities and thus different solubility parameters.[31] On blending *s*-PP with PEE*x*, the miscibility window is significantly shifted as compared to blends with *i*-PP (Figure 7). *s*-PP is miscible with PEE53-*d*−PEE73-*d* at high molecular weights but is immiscible with PEE83-*d* and PEE90-*d*. While this shift in miscibility agrees qualitatively with Bates and Fredrickson's theory[30] for conformational asymmetry, it is not quantitatively accurate, as our experiments indicate that both PE and PEE*x*'s containing 46% or less EE are immiscible with *s*-PP, although their statistical segment lengths are close to that of *s*-PP. This suggests that *s*-PP may form irregular blends with PEE*x*, as categorized by Graessley. When we consider the experimentally determined solubility parameters of the two tactic polypropylenes,[31] we see a difference in δ of approximately 0.5 $MPa^{1/2}$, with that of *s*-PP being greater as measured by PVT experiments. Assuming that δ for *a*-PP and *i*-PP are similar, as was measured by Maier et al.,[31] the miscibility window should shift in PEE*x* composition an amount corresponding to the difference in solubility parameter. Using Graessley's scale based on PEE97 as a reference point, the solubility parameter of PEE*x* increases as *x* decreases.[32] Combining these two sets of measurements, PEE83 should have a solubility parameter close to *a*-PP, while PEE52 should have a solubility parameter similar to *s*-PP. In fact, we have shown that the miscibility window for *i*-PP is centered near PEE83. However, our measurements indicate that the miscibility window for *s*-PP is centered at PEE63, somewhat higher than expected. This shift cannot be explained in terms of deuterium-labeling effects, since deuterium labeling typically leads to a decrease in δ. Thus, while the shift is qualitatively correct, additional irregular contributions must be present.

In addition to miscibility differences, the melt rheology of *i*-PP and *s*-PP has recently been shown by

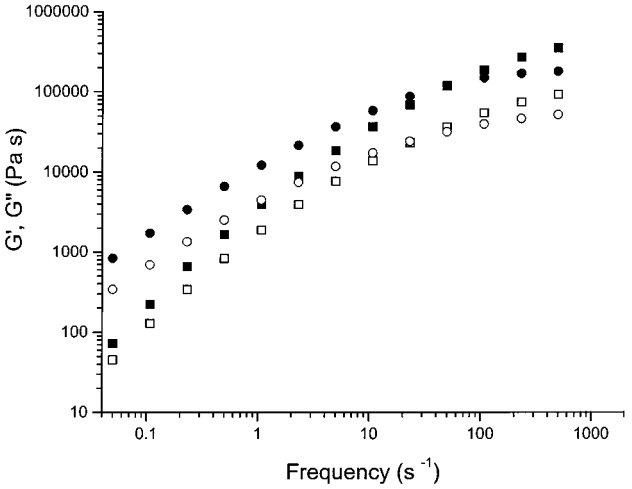

Figure 8. Comparative rheology of *s*-PP and *i*-PP. Squares represent *G′*, while circles represent *G″*. As indicated in the figure, the moduli of the *s*-PP (●, ○) are significantly higher than those of the *i*-PP (■, □) across the entire range. The plateau modulus of *s*-PP will thus be significantly higher than that of *i*-PP, as has been reported in the literature.[16]

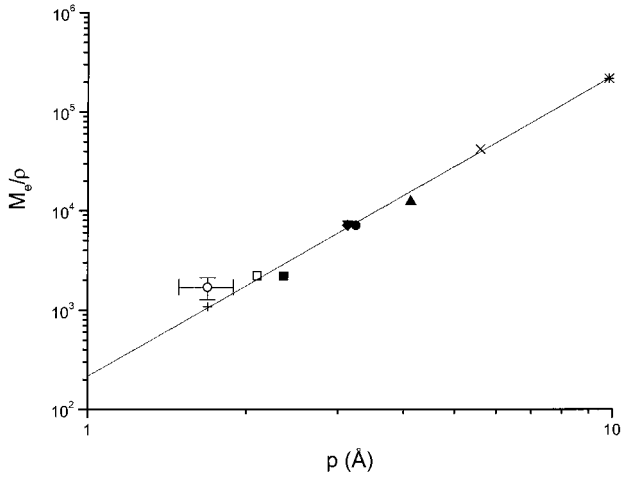

Figure 9. Comparison of *s*-PP chain dimensions with Fetters' correlation. The solid line represents the equation proposed by Fetters[9] to represent polymers at all temperatures for the relationship between entanglement molecular weight M_e and packing tube diameter *p*. The solid data points represent some of the simple polyolefins examined in the paper by Fetters et al.[11] These polymers include hydrogenated polyisoprene of various microstructures (■, ●, ▲), atactic polypropylene (▼), isotactic polypropylene (◆), polyethylene (+), atactic poly(cyclohexylethylene) (×), and poly(hexadecane) (*). The open square (□) represents the value for *s*-PP calculated from Eckstein's plateau modulus[14] and the statistical segment length measured from mixtures of *s*-PPh and *s*-PPd. The open circle (○) represents the value for *s*-PP, calculated from our estimated plateau modulus and the statistical segment length determined using the "polymer solvent" method.

Eckstein et al.[16] to be very different. Syndiotactic PP has a much greater plateau modulus and thus a lower entanglement molecular weight, M_e, and higher statistical segment length than the isotactic PP. Although we were unable to directly measure the plateau modulus for our polymer, our own rheological measurements on PP4062 and *s*-PP support this observation (Figure 8). Eckstein et al. measured a maximum of 1.35×10^5 Pa for *s*-PP. The resulting plateau modulus and our statistical segment length for *s*PP can be checked against the correlation between M_e and the packing length ($p \equiv M_{seg}/(b^2 \rho N_a)$) of Fetters et al.[11] As shown in Figure 9,

the value of $M_e = 2170$ g/mol of Eckstein et al.[16] predicts a segment length of 7.6 Å in accord with our direct measurements based on the *s*-PP h/d melts. If we assume that the last two points in the G'' curve for *s*-PP establish a maximum, then a value of 1.75×10^5 Pa results. Such a maximum has been shown to scale with the plateau modulus,[33] and using the scale factor between the measured plateau modulus and the measured maximum of Eckstein et al.,[16] we estimate that our plateau modulus is $G_N^0 = 1.75 \times 10^5$ Pa. Given the difference between the results, we expect an error of approximately 25% in our estimate of $M_e = 1710$ g/mol. Combining the result with the segment length of 8.1 Å obtained from the "polymer solvent" approach yields a point on Figure 9 in semiquantitative agreement with the correlation. Thus, using values of statistical segment length from across the observed range, we confirm that our measurements are in agreement with the accepted correlation.[11]

Conclusions

We have demonstrated that molecular weight and polydispersity are important in determining the miscibility of polyolefins. In addition, tacticity plays an important role in determining not just mechanical properties[15] but also melt properties[16] and polyolefin phase behavior. We have shown that while isotactic PP has a statistical segment length of 5.6 Å, a simple change to syndiotactic structure gives polypropylene with a statistical segment length of 7.6−8.1 Å. This change in melt conformation is accompanied by a large change in melt rheology, along with a significant shift in its miscibility with PEE*x* to lower EE contents. These results emphasize the importance of tacticity and chain packing in attempts to theoretically describe polyolefin blend thermodynamics.

Acknowledgment. The research at Oak Ridge was supported by the U.S. Department of Energy, Division of Materials Sciences, under Contract DE-AC05-00OR22725 with the Oak Ridge National Laboratory, managed by UT-Battelle, LLC. The research at the University of Minnesota was supported by Lockheed Martin 19X-SX893V/DOE and by NSERC Canada. The research at Stanford was supported by NSF (DMR-9808677).

References and Notes

(1) In *Chem. Eng. News* **1999**, *77*, 33−73.
(2) Graessley, W. W.; Krishnamoorti, R.; Reichart, G. C.; Balsara, N. P.; Fetters, L. J.; Lohse, D. J. *Macromolecules* **1995**, *28*, 1260−1270.
(3) Graessley, W. W.; Krishnamoorti, R.; Balsara, N. P.; Fetters, L. J.; Lohse, D. J.; Schulz, D. N.; Sissano, J. A. *Macromolecules* **1994**, *27*, 2574−2579.
(4) Graessley, W. W.; Krishnamoorti, R.; Balsara, N. P.; Butera, R. J.; Fetters, L. J.; Dohse, D. J.; Schulz, D. N.; Sissano, J. A. *Macromolecules* **1994**, *27*, 3896−3901.
(5) Graessley, W. W.; Krishnamoorti, R.; Balsara, N. P.; Fetters, L. J.; Lohse, D. J.; Schulz, D. N.; Sissano, J. A. *Macromolecules* **1993**, *26*, 1137−1143.
(6) Balsara, N. P.; Fetters, L. J.; Hadjichristidis, N.; Lohse, D. J.; Han, C. C.; Graessley, W. W.; Krishnamoorti, R. *Macromolecules* **1992**, *25*, 6137−6147.
(7) Balsara, N. P. In *Physical Properties of Polymers Handbook*; Mark, J. E., Ed.; American Institute of Physics Press: Woodbury, NY, 1996.
(8) Krishnamoorti, R.; Graessley, W. W.; Fetters, L. J.; Garner, R. T.; Lohse, D. J. *Macromolecules* **1995**, *28*, 1252−1259.
(9) Krishnamoorti, R.; Graessley, W. W.; Fetters, L. J.; Garner, R. T.; Lohse, D. J. *Macromolecules* **1998**, *31*, 2312−2316.
(10) Ballard, D. G. H.; Cheshire, P.; Longman, G. W.; Schelten, J. *Polymer* **1978**, *19*, 379−385.
(11) Fetters, L. J.; Lohse, D. J.; Graessley, W. W. *J. Polym. Sci., Part B: Polym. Phys.* **1999**, *37*, 1023−1033.
(12) Weimann, P. A.; Jones, T. D.; Hillmyer, M. A.; Bates, F. S.; Londono, J. D.; Melnichenko, Y.; Wignall, G. D.; Almdal, K. *Macromolecules* **1997**, *30*, 3650−3657.
(13) Thomann, R.; Kressler, J.; Setz, S.; Wang, C.; Mülhaupt, R. *Polymer* **1996**, *37*, 2627−2634.
(14) Thomann, R.; Kressler, J.; Rudolf, B.; Mülhaupt, R. *Polymer* **1996**, *37*, 2635−2640.
(15) Uehara, H.; Yamzaki, Y.; Kanamoto, T. *Polymer* **1996**, *37*, 57−64.
(16) Eckstein, A.; Suhm, J.; Friedrich, C.; Maier, R.-D.; Sassmannshausen, J.; Bochmann, M.; Mülhaupt, R. *Macromolecules* **1998**, *31*, 1335−1340.
(17) Razavi, A.; Atwood, J. L. *J. Organomet. Chem.* **1995**, *497*, 105−111.
(18) Tulloch, A.; Mazurek, M. *J. Chem. Soc., Chem. Commun.* **1973**, 692−693.
(19) Randall, J. C. In *Carbon-13 NMR in Polymer Science*; Paiska, W. M., Ed.; American Chemical Society: Washington, DC, 1979; Vol. 103.
(20) Koehler, W. C. *Physica* (*Utrecht*) **1986**, *137B*, 320−329.
(21) Wignall, G. D.; Bates, F. S. *J. Appl. Crystallogr.* **1987**, *20*, 28−40.
(22) Dubner, W. S.; Schultz, J. M.; Wignall, G. D. *J. Appl. Crystallogr.* **1990**, *23*, 469−475.
(23) de Gennes, P. G. *Scaling Concepts in Polymer Physics*; Cornell University Press: Ithaca, NY, 1979.
(24) Higgins, J.; Benoit, H. *Polymers and Neutron Scattering*; Oxford University Press: Oxford, UK, 1994.
(25) Boué, F.; Nierlich, M.; Leibler, L. *Polymer* **1982**, *23*, 29−35.
(26) Jones, T. D. Ph.D. Thesis, University of Minnesota, 2000.
(27) Bates, F. S.; Fetters, L. J.; Wignall, G. D. *Macromolecules* **1988**, *21*, 1086−1094.
(28) Pütz, M.; Curro, J. G.; Grest, G. S. *J. Chem. Phys.* **2000**, *114*, 2847−2860.
(29) Antoniadis, S. J.; Samara, C. T.; Theodorou, D. N. *Macromolecules* **1999**, *32*, 8635−8644.
(30) Bates, F. S.; Fredrickson, G. H. *Macromolecules* **1994**, *27*, 1065−1067.
(31) Maier, R.-D.; Thomann, R.; Kressler, J.; Mülhaupt, R.; Rudolf, B. *J. Polym. Sci., Part B: Polym. Phys.* **1997**, *35*, 1135−1144.
(32) Krishnamoorti, R.; Graessley, W. W.; Balsara, N. P.; Lohse, D. J. *Macromolecules* **1994**, *27*, 3073−3081.
(33) Raju, V. R.; Menezes, E. V.; Marin, G.; Graessley, G. W.; Fetters, L. J. *Macromolecules* **1981**, *14*, 1668−1676.

MA011547G